

ferent in the two cases, and the latter agreed well with the observations. The deepening rate accelerated during the initial rise in wind stress, but decreased abruptly as  $\delta V$  was reduced during the second half of the inertial period, even though  $u_*^2$  continued to increase. They thus found no evidence of deepening driven by wind stress alone on this time scale, although turbulence generated near the surface must still have contributed to keeping the surface layer stirred.

A particularly clear-cut series of observations on convective deepening was reported by Farmer (1975). He has also given an excellent account of the related laboratory and atmospheric observations and models in the convective situation. The convection in the case considered by Farmer was driven by the density increase produced by surface heating of water, which was below the temperature of maximum density in an ice-covered lake. Thus there were no horizontal motions, and no contribution from a wind stress at the surface. From successive temperature profiles he deduced the rate of deepening, and showed that this was on average 17% greater than that corresponding to "nonpenetrative" mixing into a linear density gradient. Thus a small, but not negligible, fraction of the convective energy was used for entrainment. [The numerical values of the energy ratio derived in this and earlier studies will not be discussed here; but note that the relevance of the usual definition has been called into question by Manins and Turner (1978).]

In certain well-documented cases, models developed from that of Kraus and Turner (1967) (using a parameterization in terms of the surface wind stress and the surface buoyancy flux) have given a good prediction of the time-dependent behavior of deep surface mixed layers. Denman and Miyake (1973), for example, were able to simulate the behavior of the upper mixed layer at ocean weather station P over a 2-week period. They used observed values of the wind speed and radiation, and a fixed ratio between the surface energy input and that needed for mixing at the interface.

On the seasonal time scale, Gill and Turner (1976) have systematically compared various models with observations at a North Atlantic weather ship. They concluded that the Kraus-Turner calculation, modified to remove or reduce the penetrative convective mixing during the cooling cycle, gives the best agreement with the observed surface temperature  $T_s$  of all the models so far proposed. In particular, it correctly reproduces the phase relations between the dates of maximum heating, maximum surface temperature, and minimum depth, and it predicts a realistic hysteresis loop in a plot of  $T_s$  versus total heat content  $H$  (i.e., it properly incorporates the asymmetry between heating and cooling periods). This behavior is illustrated in figure 8.3. The model also overcomes a previous difficulty and allows the potential energy to decrease during the cool-

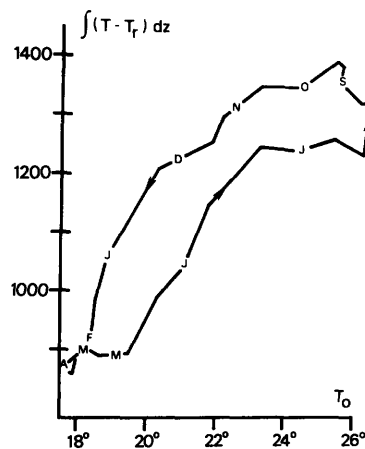


Figure 8.3 The heat content in the surface layer as a function of surface temperature  $T_0$  at ocean weather station Echo. (After Gill and Turner, 1976.) The reference temperature  $T_r$  is the mean of the temperature at 250 m and 275 m depth, and the months are marked along the curve.

ing period, instead of increasing continuously as implied by the earlier models.

The mixed-layer depth and the structure of the thermocline are not, however, well predicted by these models; this fact points again to the factors that have been neglected. Niiler (1977) has shown that improved agreement is obtained by empirically allowing the energy available for mixing to decrease as the layer depth increases [though a similar behavior is implied by the use of (8.23); see Thompson (1976) for a comparison of the two types of model]. Direct measurements of the decay of turbulent energy with depth in the mixed layer will clearly be important. In many parts of the ocean it may also be necessary to consider upwelling.

Perhaps the most important deficiency is the neglect of any mixing below the surface layer. There is now strong evidence that the density interface is never really sharp, but has below it a gradient region that is indirectly mixed by the surface stirring. At greater depths too, the density profile is observed to change more rapidly than can be accounted for by advection, so that mixing driven by internal waves, alone or in combination with a shear flow, must become significant. These internal processes are the subject of the following section.

#### 8.4 Mixing in the Interior of the Ocean

The overall properties of the main thermocline apparently can be described rather well in terms of a balance between upwelling  $w$  and turbulent diffusion  $K$  in the vertical. Munk (1966), for example, after reviewing earlier work, summarized data from the Pacific that show that the  $T$  and  $S$  distributions can be fitted by exponentials that are solutions of diffusion equations, for example

$$K \frac{d^2 T}{dz^2} - w \frac{dT}{dz} = 0, \quad (8.24)$$

with the scaleheight  $K/w \approx 1$  km. By using distributions of a decaying tracer  $^{14}\text{C}$ , he also evaluated a scale time  $K/w^2$ , and the resulting upwelling velocity  $w \approx 1.2 \text{ cm day}^{-1}$  and eddy diffusivity  $K \approx 1.3 \text{ cm}^2 \text{ s}^{-1}$  have been judged "reasonable" by modelers of the large-scale ocean circulation (chapter 15). Munk found the upwelling velocity consistent with the quantity of bottom water produced in the Antarctic, but he was not able to deduce  $K$  using any well-documented physical model. The most likely candidate seemed to be the mixing produced by breakdown of internal waves, but other possibilities are double-diffusive processes, and quasi-horizontal advection following vertical mixing in limited regions (such as near boundaries or across fronts).

Some progress has been made in each of these areas in the past 10 years, and they will be reviewed in turn. First, however, we shall discuss a set of interrelated ideas about the energetics of the process that are vital to the understanding of all types of mixing in a stratified fluid.

#### 8.4.1 Mechanical Mixing Processes

**(a) Energy Constraints on Mixing** The overall Richardson number  $Ri_0$  [defined by equation (8.8)] based on the velocity and density differences over the whole depth of the ocean, is typically very large, implying that the associated flow is dynamically very stable. But a second important fact is that the profiles of density (and other properties) are now known to be very nonuniform, with nearly homogeneous layers separated by interfaces where the gradients are much larger. Is it possible that a discontinuous structure of this kind (figure 8.4) is less stable, allowing turbulence to exist when it could not do so in the smooth average conditions?

Part of the answer was given by Stewart (1969), whose argument was developed by Turner (1973a, chapter 10). It can be shown that nonuniform profiles (different for velocity and density) can be chosen such that any value of the gradient Richardson number is attained everywhere in the interior, whatever the value of  $Ri_0$ —essentially because

$$(\Delta U / \Delta z)^2 \leq \overline{(\partial u / \partial z)^2}. \quad (8.25)$$

Thus a redistribution of properties can always reduce the gradient  $Ri$  to a value at which turbulence can be maintained.

But a crucial question remains: how is this redistribution actually produced? Consider the energy changes associated with a transition from linear gradients of velocity and density  $u = \alpha z$ ,  $\rho = -\beta z + \rho_0$  say, to a well-mixed layer of depth  $H$  (see figure 8.4). The change

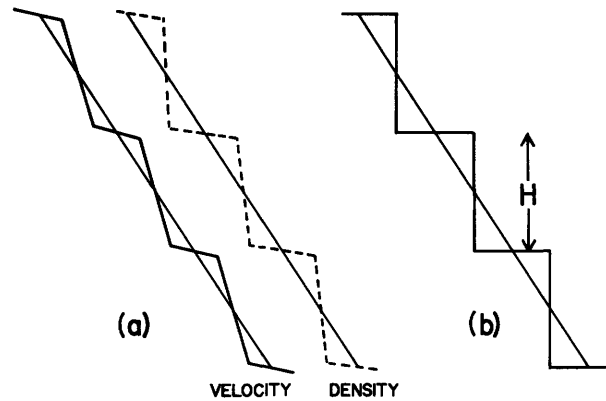


Figure 8.4 Discontinuous profiles produced by mixing, from initially linear density and velocity distributions. In (a) the final profiles, different for density and velocity, correspond to a constant gradient Richardson number everywhere, and (b) is the simpler model of homogeneous layers and thin interfaces used to derive (8.26).

in kinetic energy is  $(1/24)\alpha^2 H^3$  and in potential energy  $(1/12)g\beta H^3$ ; the two are equal when

$$Ri_0 = g\beta/\alpha^2 = 1/2. \quad (8.26)$$

This argument implies that for all  $Ri_0 \gg 1$  there is not enough kinetic energy in the local mean motion to produce the observed, nonuniform profiles, even when dissipation is neglected entirely. In the absence of sources of convective energy due to double-diffusive processes (see section 8.4.2), the general conclusion is inescapable: extra energy must be propagated into the region from the boundaries in the form of inertial or internal gravity waves if mixing is to be sustained.

The role of internal waves and their relation to the nonuniform density structure may be approached in another way, using the argument set out by Turner (1973a, p. 137), and extensions of it. Consider a deep region of stable fluid, having linear profiles of both density and velocity through it. Suppose there is a constant stress (momentum flux)  $\tau_0 = \rho u_*^2$  and buoyancy flux  $B$  through this region, sustained by small-scale turbulent motions. Mixing occurs only with fluid immediately above and below any level, so that only the internal lengthscale  $L$  defined by (8.9) will be relevant, not the overall depth or the distance from the boundaries. It follows on dimensional grounds that

$$\frac{du}{dz} = k_1 \frac{-B}{u_*^2} = k_1 \frac{u_*}{L}, \quad (8.27)$$

$$N^2 = -\frac{g}{\rho} \frac{d\rho}{dz} = k_2^2 \frac{B^2}{u_*^4} = k_2^2 \frac{u_*^2}{L^2} \quad (8.28)$$

where  $k_1$  and  $k_2$  are constants (which have not been determined experimentally). This is thus an equilibrium, self-regulated state, in which there is a unique relation between the gradients and the fluxes. The flux

Richardson number (8.7) has a fixed value  $Rf = k_1^{-1}$ , and so does the gradient Richardson number

$$Ri = k_2^2/k_1^2 = Ri_e, \quad (8.29)$$

which has been called the equilibrium Richardson number.

Only in rather special cases can this equilibrium state be maintained—one good example is the edge of a turbulent gravity current, which is treated in section 8.5.2. When density and velocity differences are imposed over a given depth, the only equilibrium state is  $Ri_0 = Ri_e$ . If  $Ri_0 < Ri_e$ , the shear will dominate, and mixing will soon be influenced directly by the boundaries. If  $Ri_0 > Ri_e$ , as it is in the case of most interest here, then the stratification will dominate, though we have already seen how a nonuniform stratification allows the local  $Ri$  to be much smaller than  $Ri_0$ , so that turbulence can persist.

In this nonuniform state, however, (8.27) shows that the transport of momentum by turbulent processes is much less efficient in the interfaces where  $du/dz$  is larger, and it is impossible to have constant purely turbulent fluxes of both buoyancy and momentum through the whole depth. But the existence of interfacial waves provides a complementary mechanism to transport momentum across the steep gradient regions without a corresponding increase in the buoyancy flux.

There have been other suggestions about the mechanism of formation of layers from a linear gradient that can be related to the above ideas. Posmentier (1977), extending an idea formulated by Phillips (1972), suggested that if the vertical turbulent flux of buoyancy decreases as the vertical density gradient increases, any perturbation causing an increase in the gradient will be amplified. This occurs because the local decrease in flux leads to an accumulation of mass, which increases the density gradient further. This behavior is in contrast to the more familiar case, described by an eddy diffusivity, where an increase in gradient increases the flux, thus tending to smooth out any irregularity.

Linden (1979) has recently reviewed a wide range of laboratory experiments on “mechanical” mixing across a density interface, including those that use a shear flow, or stirring with oscillating grids [cf. sections 8.3.2(a) and 8.3.2(c)], and has suggested how they can be unified in terms of an energy argument. Briefly, he has shown that as the overall Richardson number  $Ri_0$  increases from zero, the flux Richardson number  $Rf$  at first increases, reaches a maximum, and then falls as  $Ri_0$  becomes even larger (see figure 8.5). This form can most readily be understood in terms of the grid-stirring results already described in section 8.3.2(c). The rate of increase in potential energy is  $\frac{1}{2}g\Delta\rho u_e D^2$ , where  $u_e$  is the entrainment velocity, and the rate of supply of kinetic energy is  $\frac{1}{2}\rho u^3 D$ . Thus by definition

$$Rf = \frac{u_e g \Delta\rho D}{u \rho u^2} = \frac{u_e}{u} Ri_0. \quad (8.30)$$

Using the power-law fit to the experiments  $u_e/u \propto Ri_0^{-n}$ , we find

$$Rf \propto Ri_0^{1-n}. \quad (8.31)$$

In fact, the experimental results with salinity differences, described in section 8.3.2(c) imply that  $Rf$  is an increasing function of  $Ri_0$  at low  $Ri_0$  and a decreasing function at high  $Ri_0$  (when  $n = \frac{3}{2}$ ). The point where  $n = 1$  corresponds to the simple overall energy argument, with a constant fraction of the energy supply being used for mixing.

Relating this now to the earlier argument, the maximum on figure 8.5 (which is schematic, but has the same form for the grid-stirred and shear-driven experiments) corresponds to the “equilibrium” conditions, where the gradients and fluxes are in balance [equations (8.27) and (8.28)]. If there is a self-balancing mechanism operating in which the rate of energy supply is itself regulated by the mixing it produces [cf. section 8.5.2(a)], then this is the state attained. If there is an excess of mechanical energy and a weak gradient (to the left of the maximum), mixing acts throughout the depth to reduce the gradient and spread out the interface. When the density gradient is the dominant factor (to the right of the maximum), turbulence is suppressed in an interface but can remain unaffected elsewhere, so that it acts to sharpen incipient interfaces. The relation to Phillips’s and Posmentier’s stability argument becomes clear once we note that, for a fixed rate of kinetic energy supply,  $Rf$  is proportional to the buoyancy flux and  $Ri_0$  to the density gradient.

**(b) Instability of Waves in a Smoothly Stratified Fluid** Next, we consider the mechanisms of instability in a stratified fluid that can lead to local mixing, and thus produce or accentuate nonuniformities of the gradient. All of these involve waves propagating in from the boundaries, with or without a large-scale background shear set up by horizontal pressure gradients. When interfaces are already present, these will be the

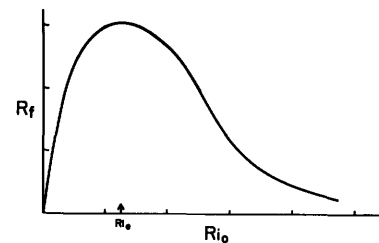


Figure 8.5 Schematic relation between the flux Richardson number  $Rf$  and the overall Richardson number  $Ri_0$  for experiments on mixing across a density interface. (After Linden, 1979.) The maximum of the curve corresponds to the “equilibrium” condition.

first regions to become unstable [see section 8.4.1(c)], but it is logical first to describe how such a structure can be set up.

It is only recently that precisely what is meant by the "breaking" of internal waves has been properly investigated (see chapter 9). Some mechanisms are clearly related to localized sources of wave energy at a nearby boundary. Lee waves can be generated by the flow over bottom topography, and when the amplitude becomes large, overturning and the production of "rotors" is possible. When the mean horizontal velocity  $u$  varies in the vertical, the "critical-layer" mechanism also leads to the growth of the waves and the local absorption of energy near the level where  $u$  equals the horizontal phase velocity of the waves (Bretherton 1966c). Small-scale "jets" attributable to this mechanism have been reported in the ocean.

Nearly always, however, the source of wave energy at a point in the interior of the ocean is not clearly identifiable, and the motion is the result of the superposition of many waves. Energy can then be concentrated in limited regions through two types of interaction. Strong interactions between an arbitrary pair of waves of large amplitude can feed energy rapidly into small-scale forced waves that overturn locally. Resonant interactions are more selective, and require two waves to be such that the sum or difference of their wavenumbers is related to the sum or difference of their frequencies by the same dispersion relation as the individual waves. These are discussed in detail by Phillips (1977a).

Various laboratory experiments have played an important part in illuminating these processes; these (and many other experiments relevant to the subject of this chapter) have been reviewed by Maxworthy and Browand (1975), and by Sherman et al. (1978). McEwan (1971) generated a single low-mode standing wave, and showed that for sufficiently large amplitudes, the original waveform became modulated with two higher modes that formed a resonant triplet with the forced wave. These grew by extracting energy from the original mode until the superposition of the several motions produced visible local disturbances of the smooth gradient, and eventually turbulent patches that were attributed to a shear-breakdown in regions of enhanced density gradient. Orlanski (1972) carried out a similar experiment, but concluded that local overturning was responsible for the production of turbulence. McEwan (1973) used two traveling internal waves of different frequency, interacting in a limited volume of an experimental tank, to examine the local conditions just before breakdown, but he was unable to say definitely whether the primary mechanism for the production of turbulence was shear breakdown or overturning.

During the experiments reported in 1971, McEwan found that patches of turbulence could also be formed

under conditions such that no resonant interaction was predicted [see also Turner (1973a, plate 24)]. More recently, this case has been studied in detail by McEwan and Robinson (1975), who explained it in terms of a "parametric" instability, which is, in fact, another resonant mechanism that had not previously been considered. This one is less selective, and gives rise to waves within a large range of much shorter wavelengths than the forcing wave, as follows. The original long wave produces a modulation of the effective component of gravity acting on shorter waves propagating through the same volume of fluid. When the forcing frequency is nearly twice the frequency of the growing disturbance, energy is fed into this disturbance through a mechanism analogous to that which causes the sideways oscillations of a pendulum to grow when the support is oscillated vertically. The major predictions of the theory, which include an estimate of the amplitude of the forcing wave required for the disturbances to overcome internal viscous dissipation and grow, were accurately verified in a most elegant laboratory experiment.

The application of this mechanism to the ocean has not yet been thoroughly tested, though McEwan and Robinson have extended Garrett and Munk's (1972a) ideas (based on their universal internal wave spectrum) to compute a mean-square slope of the isopycnals, which they deduce is large enough to excite the parametric instability. Much more work on this process is indicated; it certainly seems capable in principle of transferring energy directly from a broad range of large-scale internal waves to much smaller scales and thus creating patches of mixing in an otherwise smoothly stratified ocean.

**(c) Mixing Due to Interfacial Shears** Once sharp transition regions exist, across which both density and velocity vary markedly, it is easier to understand how local instabilities arise. The now extensive literature in this field has been well reviewed by Maxworthy and Browand (1975), and it will be treated only briefly here.

When the velocity and density profiles are similar, and the shear is gradually increased, a parallel stratified flow becomes unstable when the minimum-gradient Richardson number falls below  $1/4$ . The fastest-growing instability takes the form of regular Kelvin-Helmholtz (K-H) "billows," with a wavelength that can be predicted knowing the profiles, and that is about six times the interface thickness. Experiments by Thorpe (1971) (see figure 8.6) and Scotti and Corcos (1972) confirmed the linear-stability theory for this case in great detail. On the other hand, when the density profile is much thinner than that for velocity, some wavelengths are unstable at larger values of  $Ri$  and interfacial second-mode waves of another type have been observed at Richardson numbers up to 0.7.

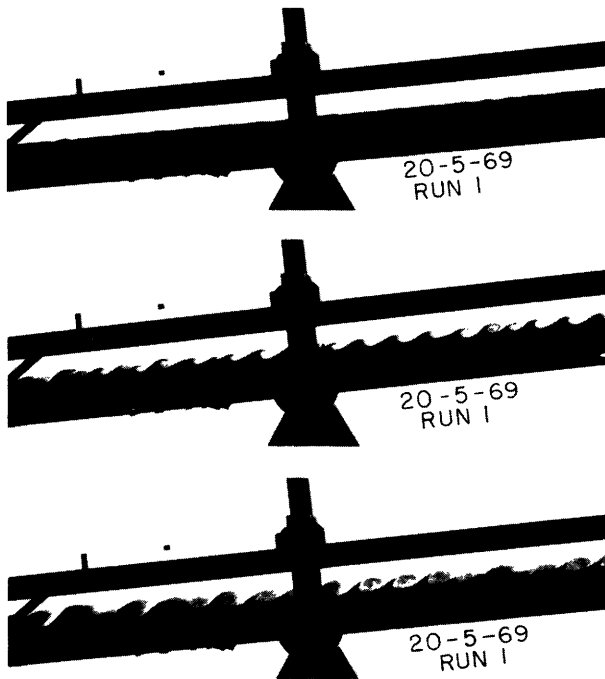


Figure 8.6 The breakdown of an interface in a shear flow to produce an array of Kelvin-Helmholtz billows. (Thorpe, 1971.)

The growth beyond the stage of initial instability has also been studied experimentally [see Thorpe (1973a) for a good review]. When the shear is increased, and then kept constant, the array of billows becomes unstable to a subharmonic disturbance, which leads to a two-dimensional rolling-up and merging of alternate vortices, a process that continues until limited by an energy constraint (as discussed below). Small-scale turbulence is produced by the concentration of vorticity into discrete lumps along the interface, and by gravitational instability within the overturned regions. The system of vortices stops growing, and then collapses, with much horizontal interleaving of mixed regions and a rapid dampening of the turbulence. This leaves behind a smoothly varying, nearly linear mean gradient of density, with thin higher gradient regions superimposed on it. Woods and Wiley (1972) suggested, however, on the basis of measurements in the ocean, that this overturning process should produce a well-mixed layer bounded by sharp interfaces. The implied “splitting” of interfaces to form new regions of high gradient does not seem to be borne out by the subsequent detailed laboratory experiments.

Thorpe (1978a) has reported observations of the mixing across the interface bounding a near-surface layer in a lake under stable conditions. Detailed measurements of temperature profiles as a function of time at one station contain all the features, including overturning and small scale mixing, described for the laboratory experiments. Thorpe concluded that the K-H instability was the dominant mechanism for mixing in

this observation period, and it is likely to be equally important in the ocean under comparable conditions.

The maximum thickening of the interface, due to mixing following the K-H instability, is limited by energy considerations closely related to those set out in section 8.4.1(a). If an initial discontinuity is transformed by this process into linear gradients of velocity and density over the same interfacial depth  $\delta$ , then equating the changes in kinetic and potential energies gives

$$\delta_{\max} = 2\rho_0 u^2 / g \Delta\rho. \quad (8.32)$$

The process is not perfectly efficient, however, and energy dissipation leads to much smaller limiting values. The numerical factor varies with the initial Richardson number of the interface, but Sherman et al. (1978) suggest using  $\delta = 0.3\rho_0 u^2 / g \Delta\rho$  as a typical value.

There are two important implications of this result. First, the instability is self-limiting. Unless the shear is increased, no further instability can occur, because the Richardson number in the thickened state is above that needed for instability. Second, the amount of vertical mixing that K-H instabilities alone can account for is small. Some other mechanism is needed to produce the turbulence in the well-mixed layers, which is essential both to transport heat and salt across them and produce the thinning of the interfaces required before further shear instabilities will be possible.

The shear needed to reduce  $Ri$  and so lead to instability at an interface can often be produced by internal waves. When a long internal wave propagates through the ocean, vorticity is concentrated at density interfaces. The sharper the interface, the more unstable it will be (i.e., the smaller the wave amplitude at which billows will form at the crests and troughs). Thorpe (1978b) has recently studied the interaction between finite-amplitude waves and an interfacial shear flow in the laboratory, and has shown that the slope at which breaking occurs can be significantly reduced. Direct visual observations of billows in the ocean generated in this way were made by Woods (1968a), using skin-diving techniques and dye tracers. Those observations had a great influence on subsequent work, by concentrating attention on the need to understand individual mixing events and processes in some detail, rather than always thinking in statistical terms. They also clearly demonstrated the relevance of simple experiments in the ocean and in the laboratory.

Recent, more sophisticated work has confirmed the importance of fine structure as a means for producing mixing in an internal wave field. Eriksen (1978) has described measurements made with an array of moored instruments, which he interprets in terms of large-scale waves “breaking.” (This paper also contains a good summary of the relevant wave theory, and references to related work.) He has shown that the appearance of

local temperature inversions (overturning) is associated with high shears, and that these are dominated by the fine-structure contribution. Moreover, there is a cutoff in the measured values of  $Ri$  at  $Ri = 1/4$ , indicating that regions with lower values of  $Ri$  are continuously becoming unstable, and implying some kind of saturation of the wave spectrum (see figure 9.28). Breaking is equally likely at any internal-wave frequency. These deductions were made using differences over 7 m, and it seems probable that the actual mixing events were unresolved at a smaller scale.

**(d) Microstructure in Turbulent Patches** The breakdown of internal waves by the mechanisms described above leaves behind a turbulent patch of fluid that tends to be thin, but very elongated in the horizontal. Such "blini" or pancakes of turbulence are distributed very intermittently in space and time, and are surrounded by fluid in which the level of fluctuations is very low. Measurements using towed instruments have shown that sometimes the turbulence is "active," i.e., there are both velocity and temperature-salinity fluctuations, but there can also be "fossil turbulence," or  $T$ - $S$  microstructure remaining after the velocity fluctuations have decayed. This specialized field can only be mentioned briefly here, though it is important enough to deserve a full-scale review [see Phillips (1977a, chapter 6)]. It has developed somewhat independently, along lines established from the statistical measurements of turbulence properties in laboratory wind tunnels and in the atmosphere, and groups in the U.S.S.R. have been particularly active [see Monin, Kamenkovich, and Kort (1974, chapter 3); Grant, Stewart, and Moilliet (1962); Gargett (1976)]. Recently, other groups have become involved, and more measurements will be summarized in section 8.4.3. In this section we just refer to two results relating to the smallest scales of motion, where the turbulence is isotropic and decaying.

For active three-dimensional turbulence to persist, it is found that the Ozmidov length scale (8.10) must be larger than about 60 times the Kolmogoroff dissipation scale  $(\nu^3/\epsilon)^{1/4}$ ; for typical conditions this implies  $L_0 \approx 1$  m. When this is so, the form of the velocity, temperature and salinity-fluctuation spectra can be predicted from the local similarity theory (Batchelor, 1959), using a scaling that does not depend on the buoyancy frequency. When an actively turbulent patch is damped by stratification, however, the form of the fossil ( $T$  or  $S$ ) turbulence is clearly affected by  $N$ , and a different scaling is appropriate. The cutoff length scale in the latter case is larger, and in principle the two can be distinguished. The important point made here, and reinforced below, is that fluctuation measurements can only be properly interpreted with a full

knowledge of various other parameters, relating to large as well as small scales.

Osborn and Cox (1972) introduced a method (which is now widely used) for estimating the vertical flux of heat from measurements of temperature fluctuations  $T'$  in the dissipation range. They suggested that there is a balance between the production of small-scale variance by turbulent velocities acting in a mean vertical-temperature gradient  $\partial\bar{T}/\partial z$  and the destruction of variance by molecular processes acting on sharpened microscale gradients. An effective vertical eddy diffusivity  $K_z$  can be defined by

$$K_z = \kappa \overline{(\partial T'/\partial z)^2} (\partial\bar{T}/\partial z)^{-2} = \kappa C, \quad (8.33)$$

where the overbar denotes an average taken over the whole record, and  $C$  has been called the Cox number. There is an uncertainty of a factor between 1 and 3 because of the unknown degree of isotropy, but there are also some more fundamental constraints on the use of this idea [e.g., see Gargett (1978)]. Particularly when there are horizontal intrusions, with associated  $T$  and  $S$  anomalies that can produce correlations between microscale temperature and salinity fluctuations (see section 8.4.3), it is not appropriate to think in terms of a gradient diffusion process based on temperature alone. Stern (1975a, chapter 11) has derived more general thermodynamic relations involving both  $T$  and  $S$  variances, but these have not yet been properly tested by detailed measurements.

## 8.4.2 Convective Mixing

**(a) Double-Diffusive Instabilities** The most dramatic change in the whole field of oceanic mixing has come about through the recognition that molecular processes can have significant effects, even on scales of motion larger than those over which molecular diffusion can act directly. It is not sufficient just to know the net density distribution: the separate contributions of  $S$  and  $T$  are also important, and when these have opposing effects on the density, the transports of the two properties are quite different, and certainly cannot be described in terms of a single eddy diffusivity. Forty years ago this was unsuspected; twenty years ago a first consequence of unequal transports was recognized but regarded as "an oceanographical curiosity" (Stommel, Arons, and Blanchard, 1956), while in recent years the examples and literature documenting coupled molecular effects has multiplied rapidly.

When temperature and salinity both increase or both decrease with depth, one of the properties is "unstably" distributed, in the hydrostatic sense. The basic fact about double-diffusive convection is that the difference in molecular diffusivities allows potential energy to be released from the component that is heavy at the top, even though the mean density distribution is hydro-

statically stable. Stommel (1962a) was one of the first to recognize that this convective source of energy implies that the potential energy is decreased, and the density difference between two vertically separated regions is increased following mixing—just the opposite to the changes occurring during mechanical mixing (see figure 8.7).

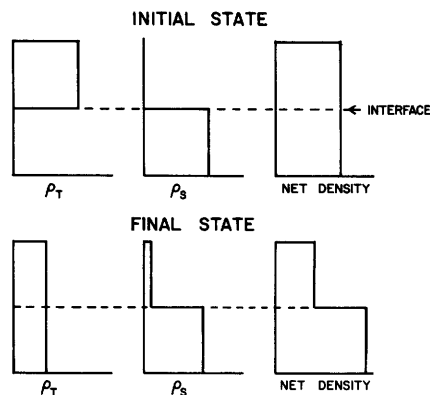
The interaction between theory and laboratory experiments on the one hand, and ocean observations on the other, has played a particularly important role in this field. The early work has been reviewed by Turner (1973a, chapter 8; 1974) and Stern (1975a, chapter 11), and more recent developments by Sherman et al. (1978). It is nevertheless worth repeating a description of two basic experiments that illustrate the different mechanisms of instability in the cases where the temperature and salinity distributions, respectively, provide the potential energy to drive the motion.

When a linear stable salinity gradient is heated from below (Turner and Stommel, 1964; Turner, 1968) the bottom boundary layer breaks down to form a convecting layer of depth  $d$  that grows in time as  $d \propto t^{1/2}$ . The experiments show that there is no discontinuity of density at the top of this layer, i.e., the temperature and salinity steps are compensating. When the thermal boundary layer ahead of the convecting region reaches a critical Rayleigh number  $Ra_c$ , it too becomes unstable. The first layer stops growing when  $d$  reaches

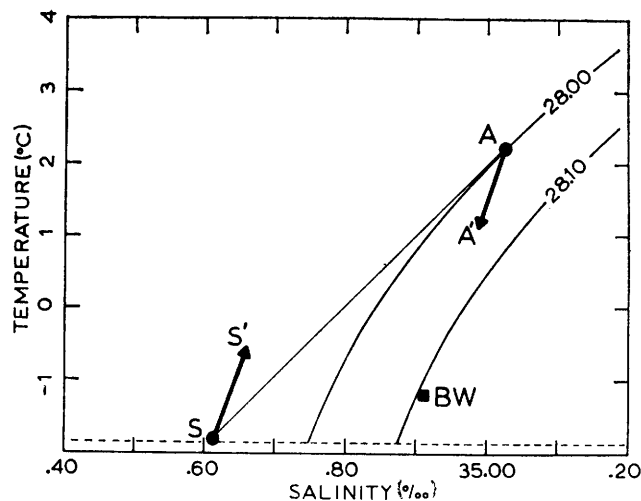
$$d_c = (\nu Ra_c / 4 K_T)^{1/4} B^{3/4} N_s^{-2}, \quad (8.34)$$

and a second convecting layer is formed. Here  $d_c$  is the critical depth,  $B = -g\alpha F_H / \rho C$  the imposed buoyancy flux corresponding to a heat flux  $F_H$  ( $\alpha$  being the coefficient of expansion and  $C$  the specific heat), and  $N_s$  the initial buoyancy frequency of the salinity distribution. Huppert and Linden (1979) recently have extended this work to describe the formation of multiple layers as heating is continued. Linden (1976) used the analog system of salt-sugar solutions to study the case where there is a destabilizing salt ( $T$ ) gradient partially compensating the stabilizing sugar ( $S$ ) gradient in the interior. He found that as the density gradients become nearly equal, the properties of the layers depend mostly on the internal properties of the gradient region, with the boundary flux just acting as a trigger. [This analog has been much used for laboratory work, since it eliminates unwanted heat losses, and more experiments using this device will be discussed later. Salt is here the analog of heat, or temperature  $T$ , since it has a higher diffusivity than sugar ( $S$ ).]

This first group of experiments illustrates well an important general consequence of opposing distributions of  $S$  and  $T$ : smooth gradients of properties are often unstable, and can break up to form a series of convecting layers, separated by sharper interfaces. In the case described, where the hotter, saltier water is



(8.7A)



(8.7B)

Figure 8.7 The changes in the separate concentrations and in the net densities produced by double-diffusion in a two-layer system: (A) schematic diagram of the initial and final properties, with a flux ratio  $\beta F_S / \alpha F_T = 0.2$ ; (B) the water properties in the Greenland Sea on a  $\theta$ - $S$  correlation diagram. (After Carmack and Aagaard, 1973.) A = Atlantic water, S = Polar water, BW = Bottom water. The double-diffusive flux alters A in direction A' and S in direction S'.

below, the convection is driven by the larger vertical flux of heat relative to salt through the "diffusive" interfaces, which are in turn kept sharpened by the convection in the layers. Many examples of such interfaces are now known in the ocean. They are distinguished from layers formed in other ways [by internal wave breaking, for instance; see section 8.4.1(b)] by the regularity of the steps and the systematic increase of both  $S$  and  $T$  with depth. For example, Neshyba, Neal, and Denner (1971) have observed such layers under a drifting ice island in the Arctic; they have been found in various lakes that are hotter and saltier near the bottom (Hoare, 1968; Newman, 1976; see figure 8.8), and they occur in various Deeps in the Red Sea (Degens and Ross, 1969).

Now consider the second type of double-diffusive process, that for which the potential energy comes from the salinity distribution (or, more generally, from the component having the *lower* molecular diffusivity). When a small amount of hot, salty water is poured on top of cooler, fresh water, long narrow convection cells or "salt fingers" rapidly form. The alternating upward and downward motions are maintained by the more rapid horizontal diffusion of heat relative to salt, which leaves behind salinity anomalies to drive the motion. The form of motion and the scale was predicted by Stern (1960a) using linear stability theory, and a description of the finite amplitude state has since been given by Linden (1973) and Stern (1975a).

At first sight, there is a very great difference between the finger structure and a series of horizontal convecting layers seen in the "diffusive" case, but Stern and Turner (1969) showed that layers can form in the finger case too. [See also Linden (1978) for a recent experiment of this kind.] A sufficiently large flux of  $S$  acting on a smooth gradient of  $T$  can cause a deep field of salt fingers to break down into a series of convecting layers, with fingers confined to the interfaces. The mechanism appears to be a "collective instability" (Stern 1969), feeding potential energy from the salt fingers into a large-scale nearly horizontal wave motion that grows in amplitude and leads to overturning. When viewed on the scale of the convecting layers, there is a close correspondence between the two cases; an unstable buoyancy flux across a statically stable interface drives convection in layers, and only the mechanism of interfacial transport differs. Many examples of layering in the ocean due to the fingering process are now known, and they often occur under warm, salty intrusions of one water mass into another. The first observations were made by Tait and Howe (1968, 1971) under the Mediterranean outflow, and a summary of other measurements is given by Fedorov (1976). The direct detection of salt fingers in the interfaces between convecting layers using an optical method (Williams,

1974a, 1975) and conductivity probes (Magnell, 1976) has now given strong support to these ideas.

Another kind of instability that is potentially important is the merging of double-diffusive layers once they have formed. Turner and Chen (1974) and Linden (1976) have shown that this can occur either by the migration of an interface, so that one layer grows at the expense of its neighbor, or by a breakdown of an interface without migration. The possibility of merging implies that one cannot always interpret observed layer scales in terms of the initial mechanism of formation—subsequent events may have changed that scale. Recent theoretical and laboratory work on double-diffusive instabilities, including finite-amplitude effects, has been summarized by Sherman et al. (1978). Much of this has continued to concentrate on one-dimensional effects, though it is difficult to find situations in the ocean where one can be sure that the *formation* of layers and interfaces has been the result of one-dimensional processes. Nevertheless, as is discussed in section 8.4.2(c), the fluxes through such interfaces can probably be adequately described in these terms. The strongest layering is associated with large horizontal gradients of temperature and salinity, and the work that takes this fact explicitly into account will now be presented.

**(b) Two- and Three-Dimensional Effects** It became clear in early laboratory experiments that layers are readily produced in a smooth salinity gradient if it is heated from the side. Thorpe, Hutt, and Soulsby (1969) and Chen, Briggs, and Wirtz (1971) showed that a series of layers forms simultaneously at all levels by the following mechanism. A thermal boundary layer grows by conduction at the heated wall, and begins to rise. Salt is lifted to a level where the net density is close to that in the interior, and fluid flows away from the wall. The layer thickness is close to

$$l = \frac{\alpha \Delta T}{\beta dS/dz}, \quad (8.35)$$

the height to which a fluid element with temperature difference  $\Delta T$  would rise in the initial salinity gradient. More recent work has shown that similar layers are formed when the salinity as well as the temperature of the vertical boundary does not match that in the interior, for example, when a block of ice is inserted into a salinity gradient and allowed to melt. Huppert and Turner (1978) have demonstrated that when there is a salinity gradient in the environment, the melt water also spreads out into layers in the interior rather than rising to the surface. This will clearly influence the way icebergs affect the water structure in the Antarctic Ocean, and it also needs to be taken into account when assessing the feasibility of using towed icebergs as a source of fresh water.

Various two-dimensional processes were explored by Turner and Chen (1974) using a tank stratified with opposing vertical gradients of sugar and salt. When an inclined boundary is inserted into a stable "diffusive" system [i.e., one having a maximum salt ( $T$ ) concentration at the top, and a maximum of sugar ( $S$ ) at the bottom], a series of layers forms by a closely related mechanism to that of side-wall heating. Both depend on there being a mismatch between conditions at the boundary and in the interior, and again a series of extending "noses" forms, and extends out into the interior. With countergradients in the "finger" sense, disturbances can propagate much more rapidly across the tank in the form of a wave motion, which leads to nearly simultaneous overturning and convection by a mechanism reminiscent of Stern's (1969) collective instability.

The intrusion of one fluid into a gradient of another has been treated explicitly by Turner (1978). The basic intrusion process with which other phenomena can be compared is the two-dimensional flow of a uniform fluid at its own density level into a linear gradient (buoyancy frequency  $N$ ) of the same property  $S$ , for example, salt solution into a salinity gradient. In that case, detailed studies (Maxworthy and Browand, 1975; Manins, 1976; Imberger, Thompson, and Fandry, 1976) show that the intruding fluid remains confined to a thin layer by the density gradient (see figure 8.9). For large Reynolds numbers, there is a balance between inertia and buoyancy forces, and the velocity  $U$  of the nose is constant, at

$$U \propto Q^{1/2} N^{1/2}, \quad (8.36)$$

where  $Q$  is the volume flux per unit width. At later stages, viscosity dominates and

$$U \propto N^{1/3} Q^{2/3} \nu^{-1/6} t^{-1/6} \quad (8.37)$$

(where  $\nu$  is the kinematic viscosity), so the velocity decreases in time. These results can be used to describe the flow into the interior of fluid mixed by processes occurring near solid boundaries (section 8.5.4). The related unsteady process, the collapse of a fixed volume of homogeneous fluid into a density gradient, has been studied by Wu (1969a) and Kao (1976); this should model the subsequent spreading of an interior mixed region produced, for example, by breaking waves [section 8.4.1(b)]. Note that relatively sharp density gradients are maintained above and below the intruding fluid (because of the way it distorts the environmental density distribution), so this is another mechanism for producing and extending layered structures. Little research has been done on the corresponding three-dimensional flows, though these are worth further study. More attention should also be paid to the possible effects of rotation in limiting the amount of spreading (cf. Saunders, 1973).

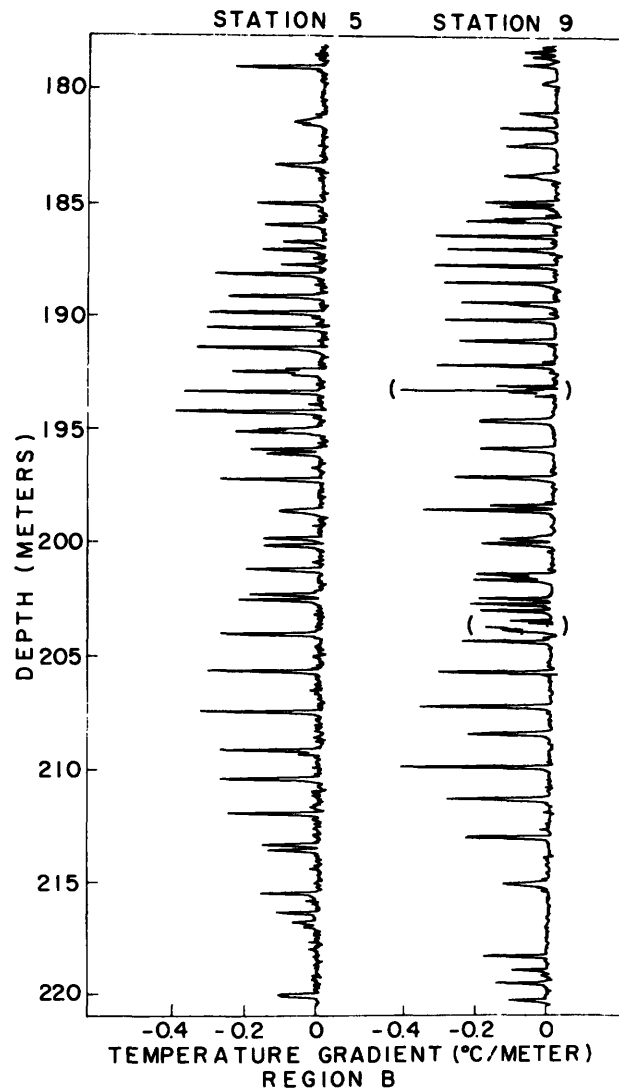


Figure 8.8 Profiles of temperature gradient recorded by Newman (1976) in Lake Kivu, showing a series of homogeneous layers separated by interfaces in which the gradient is much larger.

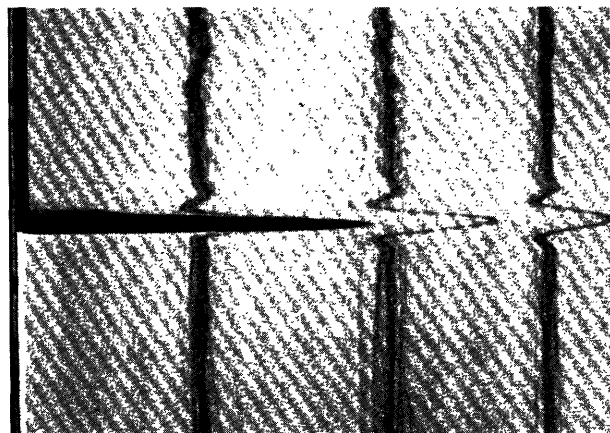


Figure 8.9 A two-dimensional intrusion of dyed salt solution into a salinity gradient at its own density level. (Turner, 1978.) Note the distortion of initially vertical dye streaks, even ahead of the injected fluid.

When the source fluid has different  $T$ - $S$  properties from its surroundings, but still the density appropriate to its depth, the behavior is very different. (The laboratory experiments were carried out using a source of sugar in a salinity gradient, but they will be described in terms of the oceanic analog of warm, salty water released into temperature-stratified fresher water.) As shown in figure 8.10, there is a strong vertical convection near the source; this is limited by the stratification, and "noses" begin to spread out at several levels above and below the source. Further layers appear, and the volume of fluid affected by mixing with the input is many times the original volume. Each individual nose as it spreads is warmer and saltier than its surroundings, so "diffusive" interfaces form above and fingers below, and there a local decrease of  $T$  or an inversion through each layer. Note too the slight upward tilt of each layer as it extends. This implies that the net buoyancy flux [see section 8.4.2(c)] through the finger interface is greater than that through the diffusive interface, so that the layer becomes lighter and moves across isopycnals. These conclusions have been supported by experiments using a source of salt in a gradient of sugar in which the sense of the interfaces, and the tilt, are just the inverse of those just described. Strong systematic shears are also associated with the layers, and the sense of these motions has been explained in terms of the horizontal density anomalies set up by the net buoyancy flux.

Another geometry of direct relevance to the ocean is a discontinuity of  $T$ - $S$  properties in the horizontal over a narrow frontal surface. In the present context, we consider only "fronts" across which the net density difference is small, and neglect rotational effects. [The larger-scale (baroclinic) instabilities that could lead to

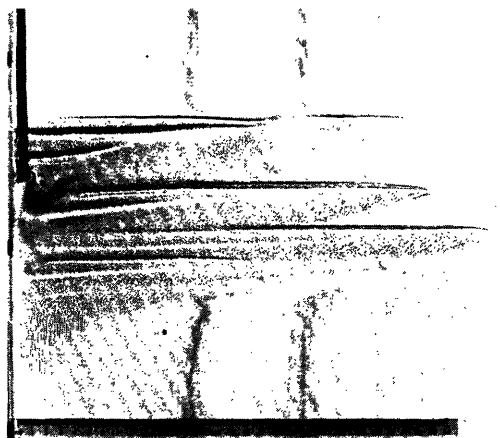


Figure 8.10 The flow produced by releasing sugar solution into a salinity gradient at its own density level. (Turner, 1978.) The gradient and the flow rate are exactly the same as for figure 8.9, but because of the double-diffusive effects, there is now strong convection and mixing near the source, followed by intrusion at several levels.

enhanced horizontal mixing in other circumstances will not be discussed here.] To model this case, Rudnick and Turner (1979) have set up identical vertical density distributions on two sides of a barrier, using sugar ( $S$ ) in one-half of a tank and salt ( $T$ ) in the other. When the barrier is withdrawn, a series of regular, interleaving layers develops (figure 8.11) whose depth and speed of advance are both proportional to the horizontal property differences, and therefore increase with depth. The scale is of the form (8.35), where  $\alpha \Delta T$  is now the horizontal anomaly across the front (though a rather different energy argument has been used to derive this result).

A general conclusion to be drawn from all the experiments just described is that the formation and propagation of interleaving double-diffusive layers is a *self-driven* process, sustained by *local* density anomalies due to the quasi-vertical transports across the interfaces. Thus, however layers have formed, whether through strictly one-dimensional processes or by interleaving, it is important to understand the mechanism and magnitude of the fluxes of  $S$  and  $T$  through them.

#### (c) Double-Diffusive Fluxes through Interfaces

Quantitative laboratory measurements have been made of the  $S$  and  $T$  fluxes across an interface between a hot, salty layer below a cold, fresh layer. They can be interpreted using an extension of well-known results for pure thermal convection at high Rayleigh number  $Ra$ . Explicitly, Turner (1965), Crapper (1975), and Marmorino and Caldwell (1976) have shown that the heat flux  $\alpha F_H$  (in density units) is well described by  $Nu \propto Ra^{1/3}$ , where  $Nu$  is the Nusselt number. This may be expressed in the form

$$\alpha F_H = A_1 (\alpha \Delta T)^{4/3}, \quad (8.38)$$

where  $A_1$  has the dimensions of a velocity. For a specified pair of diffusing substances,  $A_1$  is a function only of the ratio  $R_\rho$  of contributions of  $S$  and  $T$  to the density difference

$$R_\rho = \beta \Delta S / \alpha \Delta T, \quad (8.39)$$

where  $\beta$  is the factor relating salinity to density. When  $R_\rho < 2$ ,  $A_1 > A \approx 0.1 [g \kappa^2 / \nu]^{1/3}$ , the corresponding constant for solid boundaries, and for  $R_\rho > 2$ ,  $A_1$  falls progressively below  $A$  as  $R_\rho$  increases and more energy is used to transport salt across the interface. As discussed further by Turner (1973a), the empirical form

$$A_1 / A = 3.8 (\beta \Delta S / \alpha \Delta T)^{-2} \quad (8.40)$$

(Huppert, 1971) gives a good fit to the observations.

The salt flux also depends systematically on  $R_\rho$  and has the same dependence on  $\Delta T$  as does the heat flux. Thus the ratio of salt to heat fluxes should be a function of  $R_\rho$  alone:

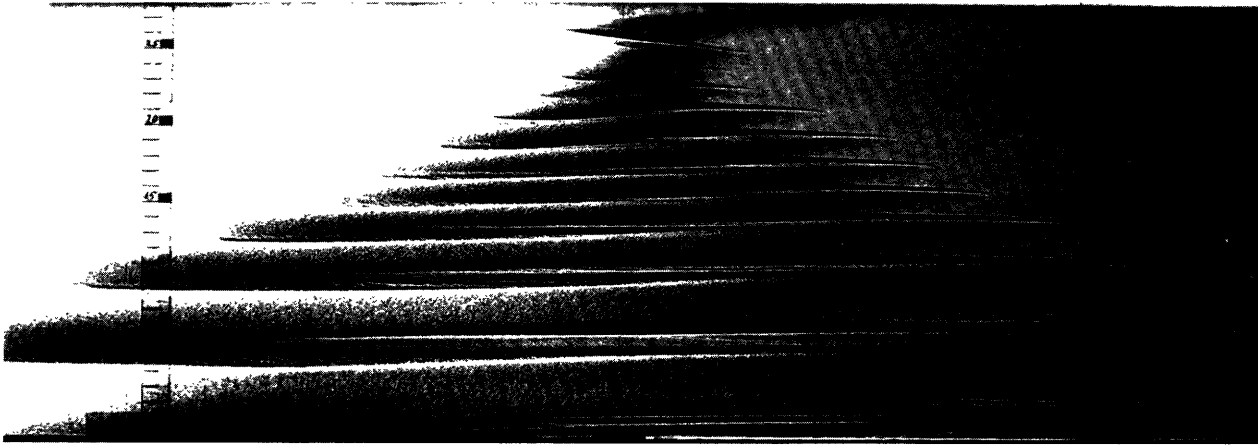


Figure 8.11 A system of interleaving layers produced by removing a barrier separating sugar solution (left) and salt so-

lution (right), which have identical linear vertical density distributions. (Ruddick and Turner, 1979.)

$$R_F = \beta F_S / \alpha F_H = f_*(\beta \Delta S / \alpha \Delta T). \quad (8.41)$$

The first two papers cited above suggest that  $R_F$  falls rapidly from unity at  $R_\rho = 1$  to 0.15 at  $R_\rho = 2$ , and then stays constant at  $R_F = 0.15 \pm 0.02$  for  $2 < R_\rho < 7$ . (It must always be less than 1 for energetic reasons, and this implies that the density difference between the two layers will always be increasing in time.) The more recent paper of Marmorino and Caldwell (1976) suggests that the flux ratio can be as high as 0.4 with much smaller heat fluxes, and also gives different values of the normalized heat flux, for reasons that are as yet unresolved. The discrepancy merits further study, since Huppert and Turner (1972) applied the earlier laboratory values to explain the temperature structure of a salt-stratified Antarctic lake, with an accuracy that seemed to make an error of a factor of two unlikely.

Linden and Shirtcliffe (1978) have extended the "thermal-burst" model of Howard (1964a) to calculate fluxes and flux ratios in the two-component case. Transports through the center of the interface are by pure molecular diffusion, while the outer edge becomes intermittently unstable when the Rayleigh number based on its thickness reaches a critical value. [This process had previously been discussed by Veronis (1968a) in a more qualitative way.] The constancy of  $R_F$  over a certain range can be predicted by assuming that boundary layers of  $T$  and  $S$  grow by diffusion to thicknesses proportional to  $\kappa_T^{1/2}$  and  $\kappa_S^{1/2}$ , and then break away together, down to the level where  $\alpha \Delta T = \beta \Delta S$ . The fluxes will then be in the ratio  $\tau^{1/2} = (\kappa_S / \kappa_T)^{1/2}$ , a result in reasonable agreement with experiments using both salt-heat and sugar-salt systems. The agreement with the individual flux measurements is much less impressive.

For finger interfaces, the condition for fingers to form in the first place has been examined by Huppert and Manins (1973). They showed that when a hot, salty

layer is placed on a cold, fresh layer (or the equivalent in the analogous system), fingers can form in the interface, as it thickens by diffusion, provided

$$\beta \Delta S / \alpha \Delta T > \tau^{3/2}. \quad (8.42)$$

Since  $\tau \approx 10^{-2}$  for heat-salt fingers, only very small destabilizing salinity differences are needed for them to form, and this suggests that salt fingers will be ubiquitous phenomena in the ocean.

Fluxes have also been measured across finger interfaces, and relations like (8.38) and (8.41) are again found to hold. Both the salt flux and the flux ratio are systematic functions of the density ratio, now more conveniently defined in the inverse sense as  $R_\rho^* = \alpha \Delta T / \beta \Delta S$ . In particular, Turner (1967) found  $\alpha F_H / \beta F_S = 0.56$  for heat-salt fingers over the range  $2 < R_\rho^* < 10$ . This result seems to be confirmed by recent work due to Schmitt (1979) and by the author (unpublished), though a much lower value of the flux ratio obtained by Linden (1973) remains unexplained. No experiments have convincingly achieved values of  $R_\rho^*$  very close to 1, where an increase in flux ratio might be expected, but this range could be of great importance for the ocean.

The experiments of Linden (1974) are also of interest. He applied a shear across a finger interface and showed that a steady shear has little effect on the fluxes, though it changes the (nearly square) fingers into two-dimensional sheets aligned down shear. Thus fluxes of  $S$  and  $T$  will be expected to persist in spite of the shears set up by interleaving motions across a front (figure 8.11). Unsteady shears, on the other hand (i.e., mechanical stirring on both sides of the interface) can rapidly disrupt the interface and decrease the salt flux.

Stern (1975a, 1976) has extended his collective-instability model (in two different ways) to describe the breakdown of fingers at the edge of an interface. He supposes that instability sets in when the salt flux

becomes too large for the existing temperature gradient, a condition that can be expressed in terms of a Reynolds number of the finger motions, and that is achieved first near the edges. This is consistent with a steady state through the interface in which the flux is

$$\beta F_S \sim C(g\kappa_T)^{1/3}(\beta\Delta S)^{4/3}, \quad (8.43)$$

where  $C$  is a function of  $R_\rho^*$  only when  $\tau = \kappa_S/\kappa_T$  is small. When  $R_\rho^* < 2$ , various laboratory experiments agree in giving  $C = 0.1$ , and this form is in better accord with experiments than previous expressions, which involved  $\kappa_S$  explicitly. Griffiths (1979) has recently proposed a model based on the intermittent growth and instability (in the Rayleigh-number sense) of the edge of an interface, the model previously applied only to diffusive interfaces. He has been able to predict a flux ratio of about 0.6, and also various properties of the fingers in the interface, including the relation between the width  $h$  and length  $L$  of the fingers ( $h \propto L^{1/4}$  approximately) that was observed by Shirtcliffe and Turner (1970) for sugar-salt fingers.

**(d) Multiple Transports through Diffusive Interfaces** It is clear from all the results described in the previous section that the "transport coefficients," defined as the vertical fluxes divided by the corresponding mean gradients, are inevitably different for heat and salt when the transports are due to double-diffusive processes acting across interfaces. For a diffusive interface, for example,

$$\frac{K_S}{K_H} = \frac{F_S}{\Delta S} \frac{\Delta T}{F_H} = R_\rho^{-1} \tau^{1/2}. \quad (8.44)$$

The effective "eddy diffusivity" of the driving (unstably distributed) component will always be larger than the driven (see figure 8.7):  $K_H > K_S$  in the diffusive case, and  $K_S > K_H$  when there are salt fingers. Both  $T$  and  $S$  are transported down their respective gradients, at different rates, but the inappropriateness of the eddy diffusivity approach becomes obvious when one considers the net density flux. This is transported against the gradient, since the potential energy is decreasing and the density difference tending to increase. Moreover, the largest individual transports occur when the density gradient is weakest, i.e., when  $R_\rho \rightarrow 1$ .

When there are several different stabilizing salts in a hot, salty layer below a cold, fresh layer, the relative transports of each across the diffusive interface can, however, be usefully described in terms of the ratio of transport coefficients  $K_i$ . Turner, Shirtcliffe, and Brewer (1970) suggested that the individual  $K_i$  can depend on the molecular diffusivities, and Griffiths (1979) has recently examined this more carefully, both theoretically and experimentally. He has predicted, using

a further extension of Linden and Shirtcliffe's (1978) "intermittent instability" model, that  $K_1/K_2$  should be proportional to  $\tau^{1/2} = (\kappa_1/\kappa_2)^{1/2}$  at low total solute-heat density ratios  $R_\rho^T$ , and to  $\tau$  at higher  $R_\rho^T$ , where a steady diffusive core dominates. The results are insensitive to the relative contributions of each component to the total density difference.

Experiments at interfacial density ratios between 2 and 4 are consistent with  $K_1/K_2 = \tau$ , but Griffiths finds an even greater separation of components at higher  $R_\rho^T$ , for reasons that are so far unexplained. The results of one of his experiments are shown in figure 8.12. He has also shown that the separation of different salts during transport through a finger interface is relatively unimportant.

These ideas have been tested on a geophysical scale using available data for Lake Kivu, a salt-stratified lake that is heated geothermally at the bottom. As illustrated in figure 8.8, this contains many well-mixed layers separated by diffusive interfaces, and Newman (1976) showed that the upward salt flux, calculated using a heat flux derived from laboratory results, is in satisfactory agreement with the salinity in the river flowing out of the top of the lake. Griffiths has used the geochemical data of Degens et al. (1973) to estimate the fluxes and gradients, and hence  $K_i$ , for several ions (potassium, sodium, and magnesium) separately. In the range  $R_\rho^T \approx 2.0$ , the effective transport coefficients decrease in order of decreasing molecular diffusivity, and the ratios are consistent with the laboratory measurements.

The above results have far-reaching, but as yet hardly explored, implications for the ocean. It is tacitly assumed that a tracer may be used to mark a water mass, and that its changing concentration is a measure of the

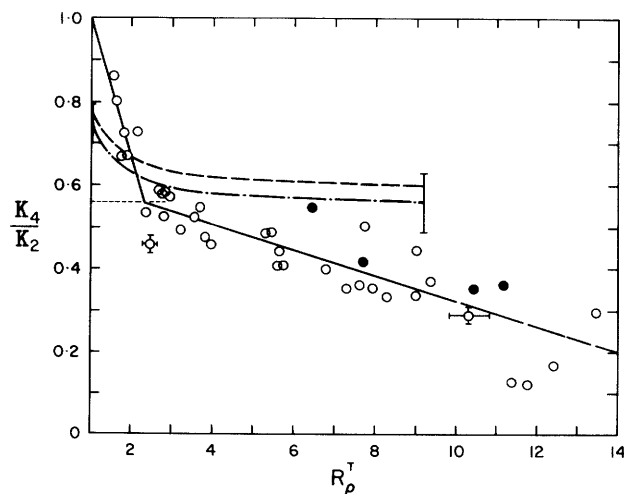


Figure 8.12 The ratio of transport coefficients for magnesium ( $K_4$ ) and potassium ( $K_2$ ) measured by Griffiths (1979) across a diffusive interface, with heating below. The ratio of molecular coefficients  $K_4/K_2 \approx 0.60$ , and the upper curves are Griffiths's theoretical predictions.

“mixing rate” for the water mass as a whole. But if diffusive interfaces are important, the transport of a tracer having a different molecular diffusivity is not necessarily a good indicator of the transport of a major component, much less of heat. In the absence of definite knowledge of the mixing mechanisms operating between the source and the sampling point, a single “eddy diffusivity” must be used with great caution.

**(e) Cabbelling and Related Instabilities** Another kind of convective instability that can lead to internal mixing depends on the nonlinear-density behavior of sea water. Particularly at low temperatures, the mixing of two parcels of water with the same density but different  $T$ - $S$  properties produces a mixture with a greater density than that of the constituents. This will sink, generating additional mixing, and the whole process is called cabbelling (various other spellings appear in the literature). Even when  $S$  and  $T$  are not quite compensating, so that the density decreases upward, a finite amplitude vertical displacement, followed by mixing, can lead to the effect described.

This possibility was first recognized at the turn of the century. Fofonoff (1956) showed that the formation of Antarctic bottom water is probably influenced by this process, and Foster (1972) has given a good account of the history, as well as a stability analysis for the case of superimposed water masses. He has applied his results to the Weddell Sea, in which the surface is generally colder and fresher than the underlying deep water. When the salinity at the surface increases due to sea-ice formation in the winter, mixtures of surface and deep water may become denser than the deep water, and thus sink through it and contribute to bottom-water formation.

Foster and Carmak (1976b) have since applied related ideas to the explanation of layers at mid-depth in the center of the Weddell Sea. They note that where the  $T$  and  $S$  gradients are weak and nearly compensating, deep well-mixed layers are formed, and they attribute this to cabbelling. But the sense of the two opposing gradients is just that required for double-diffusive instabilities to produce layers, separated by “diffusive” interfaces. At shallower depths, the gradients are larger and the layers thinner; no cabbelling instability appears to be possible, and layer formation due solely to double-diffusive effects is postulated. A closer study of the conditions separating these regimes would be instructive.

Gill (1973) has shown that when parcels of water are given finite vertical displacements, instabilities can arise due to the different compressibility of sea water at different temperatures and pressures. The compressibility of cold water is generally greater than that of warm, so in the situation discussed above, a cold parcel

displaced downward could in principle become heavier than its new surroundings. The displacements required, however, are rather large, and though the effect may be significant for bottom-water formation (see Killworth, 1977), no evidence has been found that it can influence the formation of layers in the interior, or mixing on a smaller scale.

#### 8.4.3 Observations of Fine Structure and Microstructure

There are now many observations in the deeper ocean in which the influence of the processes described in sections 8.4.1 and 8.4.2 can be identified. Most of these have been made using vertical profiles from lowered or freely falling instruments, with a few significant contributions from towed sensors [see section 8.4.1(d)]. Temperature and salinity fluctuations are the most commonly measured quantities, though small-scale velocity shear measurements are just becoming available (Simpson, 1975; Osborn, 1978).

A useful summary of the observations up to about 1974 has been given by Fedorov (1976) (with extra references in the English translation to mid-1977). He emphasizes the fine structure, or nonuniformities, of vertical gradient associated with a “layer-and-interface” structure, which needs to be known before microstructure measurements in the water column can be understood properly. The strongest layering is found near boundaries between water masses of different origin, and it is most prominent when there is a large horizontal contrast in  $T$ - $S$  but a small net density difference. Interleaving motions, with associated temperature inversions, readily develop in these circumstances, and the double-diffusive processes described in section 8.4.2(b) become especially relevant.

Only two recent examples will be cited here: profiles across the Antarctic polar front (Gordon, Georgi, and Taylor, 1977) reveal inversions that decrease in strength with increasing distance away from the front. Joyce, Zenk, and Toole (1978) have made a more detailed analysis of observations in this area, and have concluded that double-diffusive processes are significant. Coastal fronts between colder, fresh water on a continental shelf and warmer, salty water offshore also exhibit strong interleaving (Voorhis, Webb and Millard 1976). More observations and laboratory experiments related to such intrusions have been reviewed and compared by Turner (1978). It must be emphasized that double-diffusive processes can be important even in regions where the mean  $S$  increases and  $T$  decreases with depth, and both distributions are stabilizing [e.g., off the coast of California (Gregg, 1975)]. Horizontal interleaving organizes the gradients so that double-diffusive convection can act: it is a *self-driven* process, sustained by local density anomalies set up by the quasi-vertical fluxes. In this way double-diffusion

serves both to produce the layering and to dissipate the energy within it. Observations also show (Howe and Tait, 1972; Gargett, 1976) that the density gradient above a warm intrusion is typically much larger than that below, in accord with the laboratory observation of sharp diffusive interfaces above and more diffuse finger interfaces below such an intrusion.

More detailed measurements of microstructure in relation to the fine structure also show the importance of intrusions, though the interpretation of the detailed mechanism involved is sometimes ambiguous. We have already discussed [section 8.4.1(c)] the observations of Eriksen (1978), who related wave-breaking events to the fine structure, so there are certainly some occasions on which shear-generated turbulence is important. Gregg (1975) concluded from  $T$  and  $S$  microstructure profiles measured in the Pacific that the regions of most intense activity are the upper and lower boundaries of intrusions produced by interleaving, and suggested alternative explanations in terms of shear-generated turbulence and double-diffusive phenomena. The undersides of temperature-inversion layers were found to have the highest level of activity, which we can now attribute to salt fingers. Williams (1976) also found, using thermal sensors mounted on a mid-water float, that the regions of most intense mixing are closely associated with intrusive features, and he was able to distinguish occasions when one or other mechanism was dominant.

Gargett (1976) has shown that higher levels of small-scale temperature fluctuations are invariably found in areas where the vertical profiles of  $T$  and/or  $S$  have fine-structure inversions. The highest percentage of the sampled water volume was found to be turbulent when the local  $T$  and  $S$  gradients are in the finger sense. So we come back to the point made by Gargett (1978), and mentioned in section 8.4.1(d), double-diffusive processes, associated with intrusions, are very often important in producing fine structure and microstructure. Thus deductions made on the basis of temperature fluctuations alone, which, moreover, imply that the transport is entirely vertical, are not likely to be valid.

We turn now to examples of the large-scale effects of vertical double-diffusive transports across the boundaries of intrusions. Lambert and Sturges (1977) have shown that the decrease in salinity in and below the core of a warm saline intrusion can be explained in terms of the downward flux of salt in fingers. They observed a series of stable layers separated by finger interfaces, through which the flux (calculated using laboratory results) was sufficient to account for the observed rate of decrease of  $S$  with distance. Voorhis et al. (1976) used neutrally buoyant floats to record the change in  $T$  and  $S$  in the same water mass over a period of days. They found evidence of rapid vertical fluxes of

heat and salt between layers, at different rates consistent with  $\alpha F_H/\beta F_S \approx 0.5$ , approximately the laboratory value for salt fingers.

Schmitt and Evans (1978) have shown that salt fingers grow rapidly enough to survive even in an active internal wave field. They have calculated salt fluxes for measured profiles of  $S$  and  $T$ , using laboratory data and assuming that fingers are intermittently active on the high gradient regions. The calculated flux of salt is comparable to the surface input of salt due to evaporation, i.e., they deduce that fingers can account for all the vertical flux in the ocean. Carmack and Aagaard (1973) have given an example of the large-scale importance of vertical transports in the "diffusive" sense. From the changes in  $S$  and  $T$  in the deep water of the Greenland Sea, they suggest that bottom water is not formed at the sea surface, but by a subsurface modification across an interface between a colder, fresher surface layer of Polar water and a warm salty lower layer of Atlantic water (see figure 8.7B). Their deduced ratio of  $K_S/K_T \approx 0.3$ , showing that heat is definitely transported faster than salt, supports this view.

Thus, far from being an amusing curiosity, double-diffusive convection is playing a significant, and in some regions dominant, role in the vertical mixing of heat and salt in the world's oceans. Its overall importance relative to other processes such as wave breaking and boundary mixing (reviewed in the following section) has not yet been assessed adequately.

## 8.5 Mixing near the Bottom of the Ocean

Compared to that in the atmospheric boundary layer, or even the surface layers of the ocean, work on the ocean-bottom layer has been very sparse. The early research, summarized by Bowden (1962), concentrated on shallow seas, but the measurements of heat fluxes through the deep ocean bottom made it desirable to know more about the flows in those regions (Wimbush and Munk, 1970). More sophisticated instruments have now been developed to allow more detailed measurements, but as the proceedings of a recent conference on the subject show (Nihoul, 1977), there is as yet no clear consensus in this field.

### 8.5.1 Mixing Induced by Mean Currents

Most measurements of the depth of the benthic boundary layer have been referred to the "Ekman depth"

$$h_e = 0.4u_* / f, \quad (8.45)$$

which is the scale appropriate to an unstratified, turbulent flow in a rotating system. A logarithmic layer, described by (8.2), is contained within the lowest part of this, where the stress can be regarded as constant and rotation is unimportant. The Ekman theory also

predicts a veering of the current with height above the boundary.

But the data suggest (in various ways) that this may not be a directly relevant scale, because of the stable stratification of the water column. For example, figure 8.13 shows profiles of  $\theta$  and  $S$  measured by Armi and Millard (1976) on an abyssal plain. The well-mixed layer, bounded by a sharper interface, strongly suggests that this structure has been formed by stirring up the bottom part of the gradient region above (cf. figure 8.1a). This stirring is therefore an "external" mixing process, driven by turbulent energy put in at the boundary. The buoyancy flux associated with the heat flux through the bottom has a negligible effect, except when the speed of the current is very low. The layer depth  $h$  in this case is about six times  $h_e$ , and the mean depth on different days was correlated with the mean current velocity  $U$ . Armi and Millard showed that

$$F = U / \left( g \frac{\Delta\rho}{\rho} h \right)^{1/2},$$

a Froude number, was approximately constant at  $\sim 1.7$ . This led to the hypothesis that the layer depth is controlled by the instability of large-scale waves traveling along the interface. No direct evidence of such a wave-breaking process has been reported, though the temporal variation of layer depth in these and other measurements [see, e.g., Greenwalt and Gordon (1978)] indicate that waves of large amplitude are often present. Note that this Froude-number criterion is closely related to the "constant-overall-Richardson-number" hypothesis used in surface mixed-layer models [sections 8.3.2(a) and 8.3.3].

A different picture has been developed by Weatherly and van Leer (1977), on the basis of their measurements of temperature and current profiles on a continental shelf. Their boundary-layer thicknesses (defined from current profiles) were substantially smaller than (8.45), and they attributed this to the effect of stable stratification. They did, however, observe large changes of current direction in a sense consistent with Ekman veering, particularly when the stratification was large, and they have described their results in terms of a stably stratified turbulent Ekman layer. Relatively few of their profiles had well-mixed layers at the bottom, and even those suggested an advective origin, rather than local turbulent mixing. When the bottom was sloping, and the flow was along the isobaths, the observations contain a systematic increase or decrease of temperature in time, which is consistent with downwelling or upwelling along the slope produced by the Ekman transport.

It seems likely that the difference between these observations and those of Armi and Millard (1976) lies in the much weaker stratification in the deep ocean,

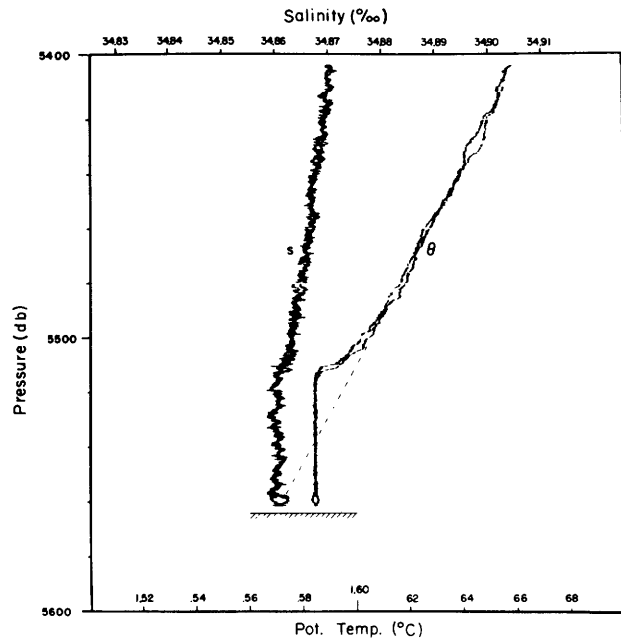


Figure 8.13 Salinity ( $S$ ) and potential temperature ( $\theta$ ) profiles measured by Armi and Millard (1976) in the middle of the Hatteras Abyssal Plain. The dashed line indicates that the structure could have formed by mixing up a stratified region above the bottom.

and the consequently larger values of  $F$  there. But before this can be regarded as certain, more measurements at other sites will be needed. Theoreticians should also look more carefully at the properties of mixed layers shallower and deeper than the Ekman depth, and systematically compare the bottom-layer results with surface mixed layers.

In shallow seas, mixing driven by turbulence produced at the bottom can extend to the surface. This tendency is counteracted by the input of heat at the surface, which produces a stabilizing temperature gradient. Qualitatively, one can see that the larger the current and the shallower the depth, the more likely is the water to be uniformly mixed for a given surface flux [cf. section 8.3.2(d)].

Simpson and Hunter (1974) showed, in fact, that there are marked frontal structures in the Irish Sea, separating well-mixed from stratified regions. The location of these fronts is determined by the parameter  $h/u^3$ , where  $h$  is the water depth and  $u$  the amplitude of the tidal stream. The choice of this form can be justified using an energy argument, related to that used to obtain (8.21). The relevant dimensionless parameter must include the buoyancy flux  $B$ , and is  $Bh/u^3$ . Thus the only extra assumption is that  $B$  varies little over the region of interest. Simpson and his coworkers have now extended this model to include the effects of wind stress as well as tidal currents, and find that this has a significant, though less important, influence.

### 8.5.2 Buoyancy-Driven Bottom Flows

(a) **Turbulent Gravity Currents** The flow of heavier water down a slope under lighter layers is important in many oceanic contexts. The density differences may be due to  $T$  and  $S$  differences, or to suspended sediment (as in turbidity currents). The velocity of such flows is strongly influenced by the mixing between the current and the water above, and mixing can determine the final destination of the flowing layer. For example, the water flowing out through the Strait of Gibraltar is denser than water at any depth in the Atlantic, but mixing with lighter water near the surface eventually makes its density equal to that of its surroundings, so that it flows out into the interior at middepth (see figure 8.14).

Turner (1973a, chapter 6) has shown how a nonrotating turbulent gravity current can be treated as a special case of a two-dimensional plume, rising vertically through its environment. [This more general problem is also relevant to the disposal of waste water in the ocean, which will not be treated here; see Koh and Brooks (1975) for a review.] The "entrainment assumption," that the rate of inflow  $u_e$  is proportional to the local mean velocity  $u$ , must be modified to take account of the stabilizing effect of buoyancy normal to the plume edge. Explicitly, it is found that

$$\frac{u_e}{u} = E(Ri_0), \quad (8.46)$$

i.e., the entrainment ratio is a function of an overall Richardson number

$$Ri_0 = \frac{g(\Delta\rho/\rho)h \cos\theta}{u^2} = \frac{A \cos\theta}{u^3}, \quad (8.47)$$

where  $h$  is the thickness of the layer,  $\theta$  the slope, and  $A = g(\Delta\rho/\rho)hu$  the buoyancy flux per unit width [cf.

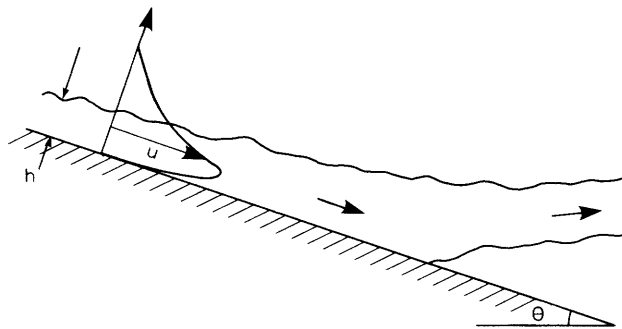


Figure 8.14 Sketch of a steady gravity current on a slope, the edge shown represents the level of most rapid variation of density. The outer part of the velocity profile sketched is linear, and so is the density profile at this level. (Ellison and Turner, 1959.) In stratified surroundings, the plume leaves the slope at a depth given by equation (8.48).

(8.8)].  $E$  is a strong function of  $Ri_0$  (see figure 8.2), and it becomes very small at low slopes.

When  $\theta$  is small, the stress across the interface is therefore negligible, and the velocity of the layer is determined by friction at the solid boundary. At high slopes, on the other hand, the stress due to entrainment dominates, and in the steady state  $u = \text{constant} \propto A^{1/3}$  from (8.47), and the rate of increase of depth with distance  $dh/dx = E$ . In this state, the turbulence is both generated and used for mixing at the interface, and this flow is thus a good example of the equilibrium "internal"-mixing process referred to in sections 8.2.1 and 8.4.1(a). The profiles of both velocity and density through the outer edge of the interface are observed to be linear, in agreement with an argument equivalent to that which led to (8.27) and (8.28) (figure 8.14).

The results for plumes rising or falling through a stratified environment can also be adapted to describe gravity currents along a slope, just by using the appropriate (smaller) value of  $E$ . For example, with a constant slope  $\theta$  and density gradient (specified by  $N$ ), the depth at which a two-dimensional current will reach the density of its surroundings and move out into the interior will be

$$Z_{\max} \propto E^{-1/3} A^{1/3} N^{-1}, \quad (8.48)$$

where  $E$  is an (empirical) function of  $\theta$ .

The effects of rotation can be added to these plume theories, and Smith (1975) described a three-dimensional rotating model that fits the observations of outflows from the Norwegian and Mediterranean Seas very well. When entrainment is dominant, rotation makes the flow tend to move along bottom contours, whereas strong bottom friction allows a larger excursion down-slope. Killworth (1977) has discussed and extended rotating two- and three-dimensional models, with the flow on the Weddell Sea continental slope in mind. In order to explain both the depth of penetration and the dilution, he also needed to include the change of buoyancy flux resulting from the increase of thermal expansion coefficient with depth.

(b) **Buoyancy Layers** In a stably stratified fluid, motions along a slope can in principle be set up by diffusion near the solid boundary, which results in the surfaces of constant concentration (of  $S$  say) being bent so as to become normal to the slope. This distortion of the density field means that fluid against the boundary will be lighter than that in the interior, and there will be an upslope flow in a thin layer where changes due to advection are balanced by diffusion. Phillips (1970) and Wunsch (1970) showed that with these boundary conditions, the thickness  $l$  and upslope velocity  $w$  are constant and given by

$$l \sim (\nu\kappa_s)^{1/4}N^{-1/2}, \quad w \sim (\nu\kappa_s)^{1/4}N^{1/2}. \quad (8.49)$$

Under laboratory conditions these are very small, but Wunsch (1970) proposed that (8.49) could be extended to oceanic slopes by using "eddy" values for  $\nu$  and  $\kappa$  rather than molecular coefficients. With  $\nu, \kappa \sim 10^4 \text{ cm}^2 \text{ s}^{-1}$ ,  $l \sim 20 \text{ m}$ ,  $w \sim 5 \text{ cm s}^{-1}$ , and more intense mixing will drive a stronger upslope current. There are several difficulties with this interpretation. It is implied that the larger mixing coefficients must be driven by some external mixing process, which is most likely to be associated with currents against the slope. This being so, it seems more appropriate to regard these "mechanical" processes as the cause, not the effect, of the near-slope motions and to investigate directly their effects on mixing. Second, the presence of two stratifying components, in the interior, with compensating effects on the density, changes the behavior markedly. As discussed in section 8.4.2(b) [see also Turner (1974)], counterflows along the slope are then produced, with much larger velocities than in the single-component case. These cannot remain steady, however, and the net result is the formation of a series of layers, extending out into the interior (cf. figure 8.10). When conditions near the slope are quiet, this mechanism could produce enhanced mixing and fine structure, but again it is likely to be overwhelmed by the mixing produced by currents.

### 8.5.3 Mixing Due to Internal Waves

Internal waves impinging on a sloping boundary can provide enough energy to cause significant mixing. The conditions under which this occurs in a continuously stratified fluid have been convincingly illustrated in the laboratory experiments of Cacchione and Wunsch (1974).

When waves of lowest mode propagate into a wedge-shaped region bounded by a solid sloping boundary and a free surface (or interface), three types of behavior are possible. These depend on the relative magnitudes of the slope  $\beta$  of the boundary and the wave-characteristic slope  $\alpha = \sin^{-1}(\omega/N)$ , which is the direction of the group velocity, and of the particle motions [see figure 8.15 and Wunsch (1969)]. If  $\beta > \alpha$ , then energy can be reflected back into the interior. If  $\beta < \alpha$ , which occurs only at sufficiently high frequencies  $\omega$  for a given  $\beta$  and stratification  $N$ , the horizontal component of the group velocity after reflexion is still directed toward the slope. Energy thus cannot escape backward, and is fed into the corner region. For example, when the deeper layers are stratified, and there is a well-mixed layer above, the amplitude will build up in the thermocline and strong local mixing can occur there. When  $\beta = \alpha$ , the particle motions become parallel to the slope, and this strong shearing motion becomes unstable to form a series of periodic vortices. Overturning

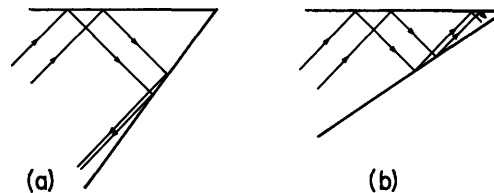


Figure 8.15 Propagation of waves into a wedge of angle  $\beta$ . The angle  $\alpha$  that rays make with the horizontal stays constant, so that when  $\beta > \alpha$  [case (a)] energy can be reflected, and when  $\beta < \alpha$  [case (b)] energy is trapped in the corner. The critical case  $\beta = \alpha$  produces strong shearing motions against the slope.

associated with these produces mixed fluid that propagates into the interior as regularly spaced layers all along the slope.

Though there is a suggestion in these and other experiments that the layer spacing is related to the amplitude of the excursion along the slope, they do not provide a definite length scale that can be used for predictions in the ocean. Nor do there yet seem to be any oceanic measurements that are detailed enough to distinguish the structure resulting from this mechanism from other possibilities.

Waves formed on density interfaces can also produce mixing when they approach a sloping boundary. For example, in a fjord that has a well-mixed surface layer and a strong pycnocline at sill depth, Stigebrandt (1976) showed that interfacial waves generated at the sill can propagate toward the landward end, where they break on the sloping shore. Using field data and a laboratory experiment, he described the vertical mixing in the lower layer in terms of this wave-breaking process, followed by the flow of mixed fluid into the interior. Similar observations have been reported by Perkin and Lewis (1978), who concluded that this mechanism probably dominates the transport between the surface and bottom layers of fjords for most of the year.

### 8.5.4 The Effect of Bottom Mixing on the Interior

There is no doubt that mixing near the bottom is much stronger than it is in the interior of the ocean. Hogg, Katz, and Sanford (1978), continuing a series of measurements near Bermuda initiated by Wunsch (1972a), recently have documented a close relation between the distribution of temperature fine structure and strong currents associated with large eddies near the island. They are cautious about identifying the precise mechanism of interaction (from among those described above, and others not discussed here), but the generation of the structure at the island slope and its decay with distance away from Bermuda is very clear.

Armi (1978) has used the contrast between vertical temperature profiles near topographic features and in the interior of an ocean basin to support one of the mechanisms for vertical mixing discussed by Munk

(1966): that the largest cross-isopycnal mixing occurs in boundary-mixed layers, and that these are then advected into the interior and so influence the structure there as well. The single well-mixed bottom layer discussed in section 8.5.1 and shown in figure 8.13 is characteristic of a smooth bottom on an abyssal plain, but over rougher topography a number of steps is often observed, suggesting bottom mixing at several depths, followed by spreading out along isopycnals that intersect the slope. The horizontal variability of such layering indicates that the process is patchy and intermittent.

The layer structure decays and the profiles become smoother as the water moves out into the interior. The various mechanisms that could play a part at this stage have been discussed in section 8.4. Some layers of water with distinctive  $T$ - $S$  properties are identifiable, however, over large distances. Armi (1978) has shown that Norwegian Sea water can be followed as a 20-m-thick layer for over 3000 km into the North Atlantic, and cites this as evidence both for large-scale advection and slow vertical mixing. Carmack and Killworth (1978) have identified a layer with anomalously low  $T$  and  $S$  characteristics that interleaves along a surface of constant potential density with Antarctic bottom water near the Ross Sea. They also suggest that the sinking of water in the form of plumes along the continental margin, followed by an outflow at mid-depth, is possible nearly everywhere round Antarctica, although water masses that are so clearly distinguishable from their surroundings are rather rare.

In summary, the available evidence supports the view that the bottom of the ocean, particularly the sloping bottom around coasts or topographic features, plays an essential role in the internal-mixing process. Near the topography, the dominant mixing mechanisms are probably mechanical, driven by large-scale currents, though gravity currents can sometimes be important. The main way in which the resulting mixed layers are carried into the interior of the ocean must be by large-scale advection, associated with processes that are nearly independent of the layers themselves. The extra spreading and interleaving due to local horizontal density anomalies [described by equations (8.36) or (8.37)] occur on a longer time scale, though these processes will also affect the final profiles in the interior. Direct vertical mixing driven by internal waves is probably active too, and bottom topography enters here in another way as a mechanism for generating the internal wave field.

The only other regions where the deduced mixing rates are comparable with those at solid boundaries are boundaries between different water masses. The evidence presented in section 8.4.3, for example, shows

that frontal surfaces with large horizontal  $T$  and  $S$  anomalies but a small net density difference are particularly active. The primary process envisaged in that case is double-diffusive transport in the vertical, producing local density anomalies that drive quasi-horizontal interleaving. Double-diffusive convection can also be significant when water masses with very different  $T$ - $S$  properties lie one on top of the other.

We conclude on a cautionary note. Though there have been rapid advances in the observation and understanding of many individual physical processes, particularly in the past 10 years, these have not yet been put together to give a satisfactory, unified picture of mixing in the ocean. We must now seek ways to distinguish between the effects of the diverse vertical and horizontal processes that have been reviewed, and to assess their relative importance in controlling the vertical distributions of temperature and salinity in the ocean as a whole.